

Discrete Change in Magnetization by Chiral Soliton Lattice Formation in the Chiral Magnet $\text{Cr}_{1/3}\text{NbS}_2$

Kazuki Tsuruta^{1*}, Masaki Mito^{1,2}, Yusuke Kousaka^{2,3}, Jun Akimitsu^{2,3}, Jun-ichiro Kishine^{2,4}, Yoshihiko Togawa^{2,5}, Hiroyuki Ohsumi^{2,6}, and Katsuya Inoue^{2,3,7}

¹Graduate School of Engineering, Kyushu Institute of Technology, Kitakyushu 804-8550, Japan

²Center for Chiral Science, Hiroshima University, Higashihiroshima, Hiroshima 739-8526, Japan

³Graduate School of Science, Hiroshima University, Higashihiroshima, Hiroshima 739-8526, Japan

⁴Graduate School of Arts and Sciences, The Open University of Japan, Chiba 261-8586, Japan

⁵Graduate School of Engineering, Osaka Prefecture University, Sakai 599-8570, Japan

⁶RIKEN SPring-8 Center, Sayo, Hyogo 679-5148, Japan

⁷Institute for Advanced Materials Research, Hiroshima University, Higashihiroshima, Hiroshima 739-8526, Japan

(Received September 12, 2015; accepted November 16, 2015; published online December 21, 2015)

In the chiral magnet $\text{Cr}_{1/3}\text{NbS}_2$, discrete changes in the magnetization (M) caused by the formation of a chiral soliton lattice (CSL) were observed in magnetization curve measurements using a single crystal of submillimeter thickness. When M is measured with a minimal increment of the magnetic field H , 0.15 Oe, discrete changes in M are observed in the H region that exhibits definite magnetic hysteresis. In particular, enormous discrete changes in M are observed as H decreases from the field above the saturation field, while fine M steps are also found in the intermediate H range independently of the sweeping direction of the field. The former is considered as a type of enormous Barkhausen effect associated with the CSL formation. The latter originates from the change in soliton number during the CSL formation.

Chirality indicates that an image in a plane mirror cannot be brought to coincide with itself, as defined by Lord Kelvin.¹⁾ For chiral materials with a broken spatial inversion, their magnetic properties are characterized by the competition between symmetric and antisymmetric Dzyaloshinskii–Moriya (DM) exchange interactions, resulting in a chiral helimagnetic structure in zero magnetic field.^{2–5)} When a magnetic field is applied perpendicular to the chiral axis of the helimagnetic structure, a type of superlattice structure called the chiral soliton lattice (CSL) becomes stabilized.⁶⁾ The pitch of CSL is controlled by applying magnetic fields. In 2012, Togawa et al. succeeded in observing CSL formation in the chiral magnet $\text{Cr}_{1/3}\text{NbS}_2$ through Lorentz microscopy and small-angle electron diffraction analysis;⁷⁾ the CSL state is robust and has phase coherence.⁷⁾ This advantage with controllability becomes more prominent when the coupling between the magnetic structure and the electron transport can be controlled. Further successful control of the phase coherence would expand the field of applications using this phenomenon.

CSL formation accompanies the creation and extinction of nodes with 2π rotations of the spin phase, namely, a “topological phase defect” or a “ 2π twist soliton”, as the magnetic field changes. Then, the magnetization should exhibit both a continuous change in magnetic moment near the phase defect and a discrete change reflecting the creation and extinction of the phase defect. Such a phenomenon has never been observed in magnetization measurements. In the case of metals with a sufficiently large mean free path for conduction electrons, they flow through an array of solitonic phase defects in the CSL, which creates a periodic scattering potential for itinerant spins. Consequently, the electrical resistance can be correlated with the number or density of solitons and thus depends on the strength of the magnetic field. Recently, a negative interlayer magnetoresistance has been observed in a bulk specimen and found to be scaled by the soliton density.⁸⁾ Moreover, discrete magnetoresistance was observed by Togawa et al. in a micro-sized sample of

$\text{Cr}_{1/3}\text{NbS}_2$ with a c -axis length of $10\text{ }\mu\text{m}$.⁹⁾ The magneto-resistance is, however, a physical quantity arising from the conduction electrons of the Nb and S atoms in the chiral magnet, so it does not directly reflect the magnetic moments of the Cr^{3+} ions making up chiral magnetic orders. If the discrete behavior of magnetization could be observed, it would become one important evidence of CSL formation.

When this type of measurement is conducted, we must distinguish the CSL formation from the Barkhausen effect, which accompanies the pinning and depinning of the domain walls.^{10,11)} The Barkhausen effect is caused by the motion of domain walls pinned in a spatially random manner. Thus, changes in magnetization (magnetization steps) resulting from domain wall motion appear randomly with respect to the sweeping of the magnetic field; they are observed in the irreversible region of the magnetization hysteresis curve.¹²⁾ In contrast, the magnetization step caused by CSL formation originates from the level crossing of the energy of the magnetic superlattice with phase coherence, so it should accompany regular steps at a fixed M with respect to changes in the magnetic field.¹³⁾ In this letter, we demonstrate the existence of a discrete change in magnetization in single crystals of $\text{Cr}_{1/3}\text{NbS}_2$ of submillimeter thickness.

$\text{Cr}_{1/3}\text{NbS}_2$ has a layered hexagonal structure of 2H-type NbS_2 intercalated with Cr atoms and belongs to the space group $P6_322$. The chiral axis of the structure is the c -axis, and its lattice parameters at room temperature are $a = 5.75\text{ }\text{\AA}$ and $c = 12.12\text{ }\text{\AA}$.^{14–16)} The periodic length of the incommensurate magnetic structure (L_{inc}) at zero magnetic field is 48 nm .¹⁾ A single crystal of $\text{Cr}_{1/3}\text{NbS}_2$ has been grown by a chemical transport technique.^{14,15)} For this experiment, we prepared a single crystal of $\text{Cr}_{1/3}\text{NbS}_2$, the volume of which (the surface area of the ab plane, S_{ab} , times the length along the c -axis, L_c) is $1.17\text{ mm}^2 \times 0.12\text{ mm}$. According to a calculation, the single crystal should contain approximately 2500 2π -rotations of spins at zero magnetic field because $L_{\text{inc}} = 48\text{ nm}$. The magnetic ordering temperature (T_c) of the present crystal is 133 K .

The magnetization (M) was measured as a function of the magnetic field strength (H) at temperatures (T) of 5 and 100 K using a superconducting quantum interference device (SQUID) magnetometer. The magnetic field was applied perpendicularly to the chiral c -axis. The increment of H was reduced to the minimum value permitted by the apparatus, 0.15 Oe. In contrast, magnetization measurements in the literature were conducted with H increments of above 1 Oe.^{8,14,16} Furthermore, in the present study, measurements were repeated five to ten times at a fixed H to improve the signal-to-noise (S/N) ratio. The diamagnetic contribution of the sample holder, which was made of epoxy resin, was subtracted from the measured magnetization, and the signal originating from the magnetization of the sample, M , is reported throughout this letter. The data of the whole magnetization process at $T = 5$ K are shown in Figs. S1–S3 of the supplemental material¹⁷ and, in the letter, we pay much attention to the results to be discussed physically.

Figures 1(a) and 1(b) show the entire M – H curves of the $\text{Cr}_{1/3}\text{NbS}_2$ crystal at $T = 5$ and 100 K, respectively. The processes of H increase and decrease are indicated by arrows. We define the critical field H_c , at which M becomes saturated and the hysteresis disappears with increasing H ; H_c was estimated to be approximately 1.9 kOe at $T = 5$ K and 1.4 kOe at $T = 100$ K. The overall behavior of the M – H curve is consistent with that reported by Miyadai et al.; M exhibits a remarkable increase just before it becomes saturated, and its H region has a definite hysteresis.¹⁴ The insets of Figs. 1(a) and 1(b) present the enlarged M – H curve just below H_c . The inset of Fig. 1(a) shows that as H decreases from H_c , three distinct steps in M appear below 1.64 kOe. The magnitude of the largest step corresponds to approximately 1% of the saturation magnetization M_s . A similar behavior was also observed at $T = 100$ K, as seen in the inset of Fig. 1(b).

We confirmed the reproducibility of the distinct M steps as H decreases from H_c via three runs, where the same measurement sequence was used for changing H . Figure 2(a) displays the data, shown in the inset of Fig. 1(a), at a different H scale ($H/H_c = 0.81$ – 0.89) corresponding to area I in Fig. 1(a). The results of the second and third runs at $T = 5$ K are presented in Figs. 2(b) and 2(c), respectively, using the same H scale as that of Fig. 2(a). In all three runs, some distinct M steps appear. The third run exhibits the largest step in M . However, the series of M steps is not perfectly reproducible in terms of both the magnitude of M steps (ΔM) and the field where the M steps appear, suggesting that a pinning site existing over the crystal affects this phenomenon.

Next, we focus on the H region near H_c . Figure 3 shows enlarged M – H curves at $T = 5$ K in the first run as H decreases (a) and increases (b) for $H/H_c = 0.86$ – 0.89 , respectively, corresponding to areas II and III in the inset of Fig. 1(a). As mentioned earlier, the change in M due to the CSL formation consists of both the continuous change (χH) near the phase defect and the discrete changes M' ($= \Sigma \Delta M$) reflecting the creation and extinction of the phase defect, i.e., $M = \chi H + M'$, where χ is the susceptibility. To find minute M steps, a linear contribution [as shown by the dashed line in Figs. 3(a) and 3(b)] against H was subtracted from the observed M . Consequently, we detect a meaningful M step, the magnitude of which exceeds the experimental scattering

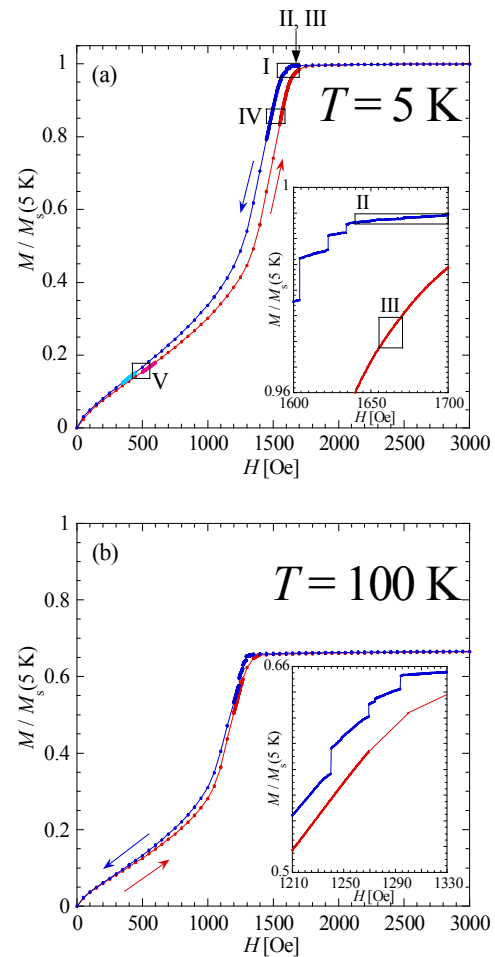


Fig. 1. (Color online) Entire M – H curves for a single crystal of $\text{Cr}_{1/3}\text{NbS}_2$ at $T =$ (a) 5 K and (b) 100 K. Insets show enlarged M – H curves at just below H_c . The processes of H increase and decrease are indicated by arrows. The region labeled by the numbers I to V is prepared in order to indicate where each figure in Figs. 2–5 corresponds in the entire magnetization curve [I: Fig. 2, II: Fig. 3(a), III: Fig. 3(b), IV: Fig. 4, and V: Fig. 5].

of 1×10^{-6} emu at maximum. Indeed, as H increases, many steps in M' are observed even just below H_c , as seen in Fig. 3(b). Figure 3(a) shows that as H decreases from H_c , several prominent M steps have already appeared, even before the appearance of the remarkable M steps seen in Figs. 1(a) and 2(a).

To discuss the nature of the discrete M steps observed in $\text{Cr}_{1/3}\text{NbS}_2$, we investigate the regularity of discrete M changes in the H region far from H_c . Figure 4(a) shows the M – H curves as H decreases ($H/H_c = 0.78$ – 0.79) and increases ($H/H_c = 0.82$ – 0.83), both of which correspond to area IV in Fig. 1(a); Fig. 4(a) covers $M/M_s = 0.85$ – 0.87 . Figure 4(b) shows the deviation obtained by subtracting the linear contribution [dashed line in Fig. 4(a)] from the observed M for decreasing and increasing H , presented as M'_1 and M'_2 , respectively. The two scales are adjusted such that $M'_1 = 1.7M'_2$. We confirm the prominent M steps in both M'_1 and M'_2 against H . The fields in which the M steps in M'_1 and M'_2 appear are marked by dotted lines in both Figs. 4(a) and 4(b). Attractive M steps are labeled with letters. For decreasing and increasing H , the equivalent M' 's are connected by green dotted lines. Careful observation reveals that most of the M' steps for increasing H are related to some

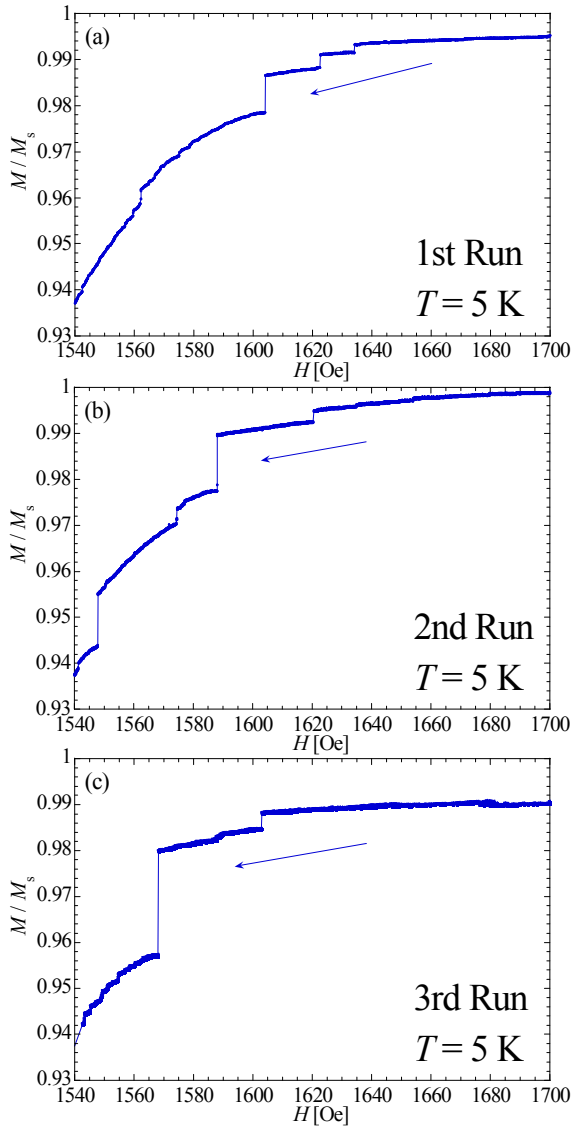


Fig. 2. (Color online) Enlarged M - H curves in the magnetic field region just below H_c as H decreases: (a) first, (b) second, and (c) third runs for $H/H_c = 0.81$ – 0.89 , corresponding to area I in Fig. 1(a). All the data in Figs. 1 and 3–5 are the results of the first run, and the data of the second and third runs appear only in Fig. 2.

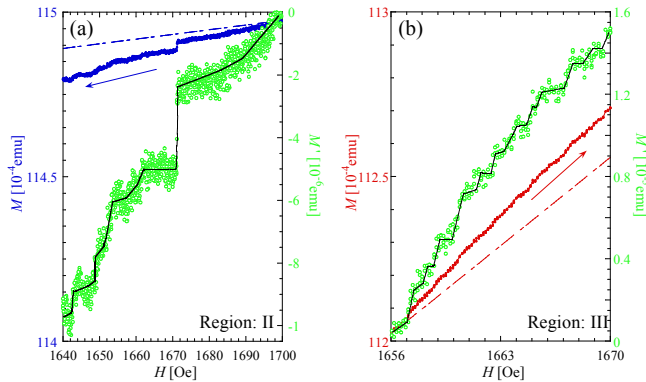


Fig. 3. (Color online) Enlarged M - H curves for (a) decreasing and (b) increasing H for $H/H_c = 0.86$ – 0.89 , corresponding to areas II and III in the inset of Fig. 1(a). The processes of H increase and decrease are indicated by arrows. To find minute M steps, a linear contribution against H (dashed line) was subtracted from the observed M . The deviation is presented as M' .

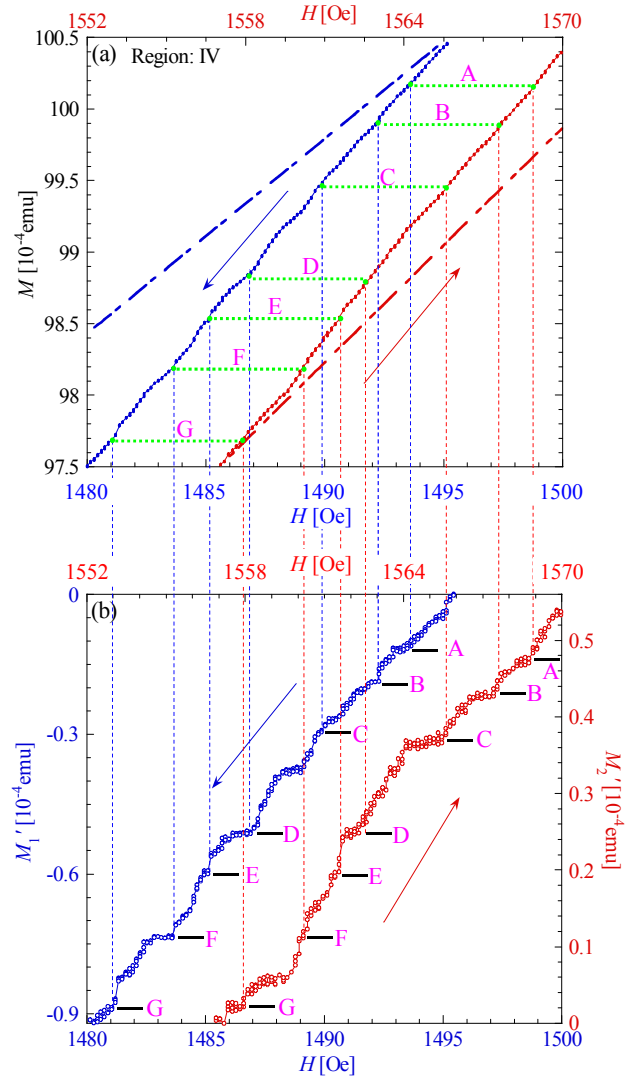


Fig. 4. (Color online) (a) Enlarged M - H curve for decreasing and increasing H for $M/M_s = 0.84$ – 0.87 , corresponding to area IV in Fig. 1(a). The processes of H increase and decrease are indicated by arrows. (b) The deviations for decreasing and increasing H obtained by subtracting the linear contribution [dashed lines in (a)] from the observed M are presented as M'_1 and M'_2 , respectively. Attractive M steps are labeled with letters. The values of χ for decreasing and increasing H are 1.4×10^{-5} and 1.8×10^{-5} emu/Oe, respectively.

of the M' steps observed for decreasing H . These M' steps are also recognized in the data of dM/dH (see Fig. S4¹⁷⁾). This regularity indicates that the series of discrete changes in M observed in $\text{Cr}_{1/3}\text{NbS}_2$ originates not from a pinning effect like the Barkhausen effect but from the intrinsic CSL formation. At $M/M_s = 0.85$ – 0.87 , the ratios of M' against the change in M for decreasing and increasing H are 33 and 20%, respectively. When the linear contribution becomes much larger, it would be difficult to find meaningful M steps.

Finally, we confirm whether M steps are observed in a field region as small as $H/H_c < 0.3$; the attractive field region is where M changes almost linearly against H and exhibits no significant hysteresis. Figure 5 shows the M - H curves for decreasing H (a) and increasing H (b) for $H/H_c = 0.22$ – 0.29 , which correspond to area V in Fig. 1(a). Here, there are no meaningful M steps for both decreasing and increasing H , suggesting that the discrete contribution reflecting only the creation and extinction of the phase defect is too small.

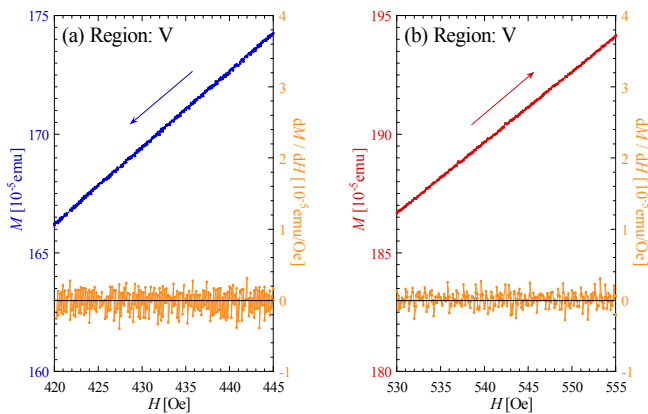


Fig. 5. (Color online) Enlarged M - H curves for (a) decreasing and (b) increasing H for $H/H_c = 0.22$ – 0.29 , corresponding to area V in Fig. 1(a). The processes of H increase and decrease are indicated by arrows. Furthermore, dM/dH is shown to identify the existence of a discrete component.

Ghimire et al. pointed out that the CSL phase can be divided into two regions in terms of the H dependence of M .¹⁶⁾ In low-field regions, M changes linearly against H , whereas, in high-field regions, dM/dH is not constant and M exhibits a large hysteresis. The present experiments show that, in the single crystal with a volume of 0.14 mm^3 , all of the observed M steps appear in the high-field region, where CSL is composed of rich ferromagnetic arrays connected to 2π twist soliton. In contrast, we did not observe any definite M steps in low-field regions, where CSL is composed of a rich spin helicity between which short ferromagnetic arrays exist. At around 1.2 kOe , the meaningful M steps begin to appear [see Figs. S2(b) and S3(c)¹⁷⁾].

According to the literature, the periodic length of the incommensurate magnetic structure (L_{inc}) at $H = 0$ is 48 nm .¹⁴⁾ This reveals that, along the c -axis, the spin phase changes from 0 to 2π radians over the span of 48 nm . As H is applied in the direction perpendicular to the c -axis, the number of the above-mentioned phase changes decreases. In the CSL state, this 2π phase rotation is considered to be a type of phase defect in the ferromagnetic spin alignment. The transformation of CSL is related to the change in the number of phase defects (n).¹³⁾ Thus, with increasing H , a decrease in n increases M . Here, the change in M due to the CSL formation consists of the continuous change (χH) near the phase defect and the discrete change M' ($= \Sigma \Delta M$) reflecting the creation and extinction of the phase defect. In theory, for a finite system, as H approaches H_c , ΔM increases, whereas the H interval in which M is constant, ΔH , decreases.¹³⁾ The present crystal is considered to be a quasi-infinite system, because it contains approximately 2500 phase defects, and indeed ΔM in the process of H increase does not exhibit a systematic increase. Thus, the experimental data are inconsistent with the theoretical H dependence of ΔM (see Fig. S5¹⁷⁾). Now, an assembly consisting of nondistinguishable ΔM 's can be evaluated with the χH term, so that the scattering of dM'/dH in the high magnetic field (ex. Fig. S4¹⁷⁾) is larger than that in the low magnetic field (ex. Fig. 5).

The change in M due to the CSL formation consists of continuous and discrete changes. If the change in M would consist only of discrete components, ΔM due to the

disappearance and/or appearance of “one phase defect” is estimated to be $5 \times 10^{-6} \text{ emu}$, which is obtained by dividing M_s by 2500 (the number of all phase defects at $H = 0$ in the present sample). For increasing H , ΔM is at most $5 \times 10^{-5} \text{ emu}$, which corresponds to at least 10 phase defects (the change in n , Δn , is 10). For decreasing H , at a certain H corresponding to approximately $H/H_c = 0.9$, ΔM corresponds to the change in $\Delta n = 25$ – 100 at least over three runs. The present measurement error N over the entire measurement is 0.01% of M_s at $T = 5 \text{ K}$, which corresponds to the change in M for $\Delta n = 1/4$. However, the existence of the linear component disturbs the detection of ΔM ($\Delta n = 1$), even if $N < \Delta M$ ($\Delta n = 1$). Indeed, for increasing H , the present lower limit at which ΔM can be detected corresponds to at least $\Delta n = 5$ because of the large linear contribution. It will be interesting to investigate the discrete change in M in the low-field regime using a micro-sized crystal, because it is considered that the linear component is small.

The M jumps due to the Barkhausen effect should generally appear randomly in the irreversible H region. In the bulky single crystal of $\text{Cr}_{1/3}\text{NbS}_2$, enormous M steps were observed as H decreased from H_c , similarly to the Barkhausen effect observed in a nanowire system.¹²⁾ This stepping reflects each M step of the transformation from the forced ferromagnetic state to successive CSL states, and the nonreproducible feature is similar to that of the Barkhausen effect. It is considered to be a type of enormous Barkhausen effect assisted by the CSL formation: We consider that the pinning due to structural defects in CSL formation cannot be ignored, especially for decreasing H . However, in the magnetic field region far from H_c , a series of discrete M changes exhibits regularity (see Fig. 4). Their characteristics cannot be understood within the framework of the Barkhausen effect. Rather, they should be understood as discrete changes in M originating from the creation and extinction of phase defects in the CSL formation, which is tuned only by the magnetic field at a constant temperature.

In principle, the number of discrete M changes is proportional to the c -axis length of the crystal (L_c). We are currently studying the size effects of varying L_c for crystals of the same quality. We must focus on the M - H data for decreasing H far from H_c . The present crystal, with a volume of 0.14 mm^3 , is quite large. To detect the M steps using a commercial SQUID magnetometer, we should not reduce the crystal size to one-tenth or less of the present size. In a previous study, the increment of magnetic field was at least 1 Oe ,^{8,14–16)} and therefore a series of discrete changes was not observed. The increment at least 0.2 Oe is necessary to detect discrete changes. For the $H \parallel c$ -axis, even M steps due to the Barkhausen effect were not observed (see Fig. S6¹⁷⁾).

Finally, we discuss the similarity between the discrete M jump due to the CSL formation and that due to the spin-slip and spin-locking observed in rare-earth metals.^{18–20)} The latter originates from the inconsistency between the in-plane magnetic anisotropy and spin helicity and, for instance, in Holmium below $T = 15 \text{ K}$, it occurs when H is applied along the helical axis.²⁰⁾ However, both accompany the discrete M jumps in magnetic hysteresis: The number of M jumps for the latter is limited to the order of ten at most. From the phenomenological perspective, both can be considered as discommensuration effects.

We observed discrete changes in M due to CSL formation in $\text{Cr}_{1/3}\text{NbS}_2$ by applying a magnetic field perpendicular to the chiral c -axis. As H decreases from H_c , the discrete changes in M become enormous and exhibit no regularity over several runs. It is a type of enormous Barkhausen effect assisted by the CSL formation, and here we must consider the effects of pinning. However, a series of discrete M changes occurs regularly in a certain field region far from H_c . These discrete changes in M originate from the change in soliton number in CSL (precisely the creation and extinction of phase defects) that is tuned by the magnetic field. These experiments show that, in a single crystal with a volume of 0.14 mm^3 , all of the observed discrete ΔM steps appear in the hysteretic H region in which the CSL with rich ferromagnetic arrays exists.

Acknowledgment This work was supported by Grants-in-Aid for Scientific Research, Grant Numbers (A) 18205023 and (S) 25220803, from the Ministry of Education, Culture, Sports, Science and Technology, Japan (MEXT).

*n590901k@mail.kyutech.jp

- 1) L. Kelvin, *Baltimore Lectures on Molecular Dynamics and the Wave Theory of Light* (C. J. Clay and Sons, London, 1904) p. 619.
- 2) I. E. Dzyaloshinskii, *Sov. Phys. JETP* **5**, 1259 (1957).
- 3) I. Dzyaloshinsky, *J. Phys. Chem. Solids* **4**, 241 (1958).

- 4) T. Moriya, *Phys. Rev.* **120**, 91 (1960).
- 5) T. Moriya, *Phys. Rev. Lett.* **4**, 228 (1960).
- 6) J. Kishine, K. Inoue, and Y. Yoshida, *Prog. Theor. Phys. Suppl.* **159**, 82 (2005).
- 7) Y. Togawa, T. Koyama, K. Takayanagi, S. Mori, Y. Kousaka, J. Akimitsu, S. Nishihara, K. Inoue, A. S. Ovchinnikov, and J. Kishine, *Phys. Rev. Lett.* **108**, 107202 (2012).
- 8) Y. Togawa, Y. Kousaka, S. Nishihara, K. Inoue, J. Akimitsu, A. S. Ovchinnikov, and J. Kishine, *Phys. Rev. Lett.* **111**, 197204 (2013).
- 9) Y. Togawa, T. Koyama, Y. Nishimori, Y. Matsumoto, S. McVitie, D. McGrouther, R. L. Stamps, Y. Kousaka, J. Akimitsu, S. Nishihara, K. Inoue, I. G. Bostrem, V. E. Sinitsyn, A. S. Ovchinnikov, and J. Kishine, to be published in *Phys. Rev. B*.
- 10) H. Barkhausen, *Z. Phys.* **20**, 401 (1919).
- 11) R. M. Bozorth and J. F. Dillinger, *Nature* **127**, 777 (1931).
- 12) E. Puppini, *Phys. Rev. Lett.* **84**, 5415 (2000).
- 13) J. Kishine, I. G. Bostrem, A. S. Ovchinnikov, and V. E. Sinitsyn, *Phys. Rev. B* **89**, 014419 (2014).
- 14) T. Miyadai, K. Kikuchi, H. Kondo, S. Sakka, M. Arai, and Y. Ishikawa, *J. Phys. Soc. Jpn.* **52**, 1394 (1983).
- 15) Y. Kousaka, Y. Nakao, J. Kishine, M. Akita, K. Inoue, and J. Akimitsu, *Nucl. Instrum. Methods Phys. Res., Sect. A* **600**, 250 (2009).
- 16) N. Ghimire, M. McGuire, D. Parker, B. Sipos, S. Tang, J.-Q. Yan, B. Sales, and D. Mandrus, *Phys. Rev. B* **87**, 104403 (2013).
- 17) Supplemental material.
- 18) J. Jensen, *Phys. Rev. B* **54**, 4021 (1996).
- 19) D. Gibbs, D. E. Moncton, K. L. D'Amico, J. Bohr, and B. H. Grier, *Phys. Rev. Lett.* **55**, 234 (1985).
- 20) R. A. Cowley, D. A. Jehan, D. F. McMorrow, and G. J. McIntyre, *Phys. Rev. Lett.* **66**, 1521 (1991).